Modeling of self-excited dust vortices in complex plasmas under microgravity

M. R. Akdim and W. J. Goedheer*

FOM Institute for Plasmaphysics "Rijnhuizen," Association EURATOM-FOM, P.O. Box 1207, 3430 BE Nieuwegein, The Netherlands

(Received 2 September 2002; revised manuscript received 26 February 2003; published 23 May 2003)

A two-dimensional hydrodynamic model for a dusty argon plasma in which the plasma and dust parameters are solved self-consistently has been supplemented with a separate dust particle tracing module to study the behavior of dust vortices. These coherent vortices appear in plasma crystal experiments performed under microgravity conditions. The nonconservative total force exerted by the discharge on the dust particles is responsible for the generation of the vortices. The contribution of the thermophoretic force driven by the gas temperature gradient plays an insignificant role in the generation of the vortices, even when the gas heating via the dust particles is taken into account. The forces related to the electric field, including the ion drag force, are dominant.

DOI: 10.1103/PhysRevE.67.056405 PACS number(s): 52.27.Lw, 52.25.Vy, 52.65.−y

INTRODUCTION

Plasma crystal experiments performed under microgravity conditions have shown dust vortices which usually appear outside the crystalline regions. In their PKE (Plasmakristall-Experiment) chamber (Fig. 1) Morfill *et al.* usually observed two stable dust vortices near the edges of the electrodes (Fig. 2), one rotating clockwise and the other counterclockwise [1,2].

Other authors have reported various theoretical and numerical studies of the driving mechanisms behind these vortices [3,4]. None of these, however, fully explain the mechanism behind their creation under microgravity.

Theoretical and numerical studies up to now have basically followed dust particles in the electric field and particle fluxes of an undisturbed discharge. An important aspect not covered is the influence of the dust on the discharge. For this, a fully self-consistent model is needed. We have developed such a model for a dust containing radio frequency (rf) discharge in argon and used it to investigate the behavior of dust particles. The model contains a dust-argon fluid part which has been described in a previous article [5] and an additional part that takes the inertia and the screened Coulomb interaction between the dust particles into account to trace dust particles in a dusty argon discharge. In existing models [6,7], the influence of the dust particles on the discharge due to recombination on their surface or the motion of the dust is neglected. If a discharge contains a considerable amount of dust, as in the PKE experiments, this approximation is not correct. Our model accounts for the influence of the dust fluid on the plasma and for its transport as a fluid. This makes it a sophisticated tool for studying dusty discharges. The dust-argon fluid model provides the input data for a separate module which calculates the dust particle trajectories in the force field present in a dusty discharge. In this paper we describe the particle tracing module and the results obtained with it, studying in particular the generation of vortices.

*Email address: goedheer@rijnh.nl

FLUID MODEL

In the fluid part of our two-dimensional model, the particle balances, the electron energy balance, and the Poisson equation are solved, including the transport of the dust fluid. For each particle a density balance can be written as

$$\frac{dn_j}{dt}+\vec{\nabla}\cdot\vec{\Gamma}_j=S_j, \tag{1}$$

where n_j is the particle's density, $\vec{\Gamma}_j$ the flux of the species, and S_j the sink or source terms.

The momentum balance is replaced by the drift-diffusion approximation, where the particle flux consist of a diffusive term and a drift term,

$$\vec{\Gamma}_j=\mu_j n_j\vec{E}-D_j\vec{\nabla}n_j, \tag{2}$$

where μ_j and D_j are the mobility and diffusion coefficient of species j. $\vec{E}$ is the electric field.

The flux of the dust particles can also be written as a drift-diffusion expression. Setting the friction force exerted by the neutral gas equal to the sum of the other forces, including the force term from the dust pressure gradient, results in

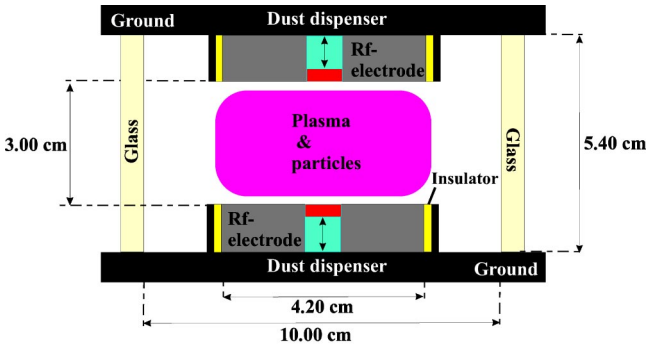

FIG. 1. A schematic diagram of the PKE chamber.

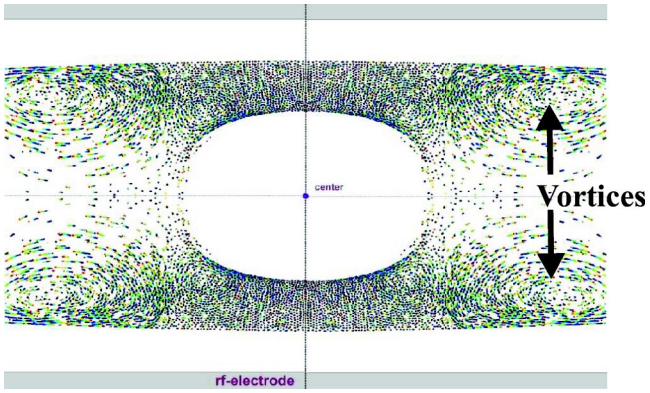

FIG. 2. A dust crystal in a PKE experiment under microgravity conditions [2]. The vortices usually appear at the outer edges.

$$\vec{\Gamma}_d = \frac{\sum \vec{F}_d}{m_d \nu_{md}} - \frac{k_B T_d}{m_d \nu_{md}} \vec{\nabla} n_d, \tag{3}$$

with m_d the mass of the dust particle and ν_{md} the momentum loss frequency due to friction. The diffusion coefficient is enhanced at high dust densities in order to model the crystal formation [5].

For ions the characteristic momentum transfer frequency is only a few megahertz. To use the drift-diffusion approximation for ions for rf frequencies higher than a few megahertz the electric field in Eq. (2) is replaced by an effective electric field; by using this effective electric field $\vec{E}_{eff}$, inertia effects are taken into account [8].

The electric field $\vec{E}$ and potential V are calculated using the Poisson equation:

$$\Delta V = -\frac{e}{\epsilon_0}(n_i - n_e - Q_d n_d), \tag{4}$$

$$\vec{E} = -\vec{\nabla} V, \tag{5}$$

where e is the elementary charge, ϵ_0 the permittivity of vacuum space, n_e the electron density, n_i the ion density, Q_d the charge on a dust particle, and n_d the dust density.

The electron energy density $w_e = n_e \epsilon$ (i.e., the product of the electron density and average electron energy ϵ) is calculated self-consistently from the second moment of the Boltzmann equation:

$$\frac{dw_e}{dt} + \vec{\nabla} \cdot \vec{\Gamma}_w = -e\vec{\Gamma}_e \cdot \vec{E} + S_w, \tag{6}$$

where $\vec{\Gamma}_w$ is the electron energy density flux:

$$\vec{\Gamma}_w = \frac{5}{3}\mu_e w_e \vec{E} - \frac{5}{3} D_e \vec{\nabla} w_e, \tag{7}$$

and μ_e and D_e are the electron mobility and electron diffusion coefficients. The term S_w in the electron energy balance equation is the loss of electron energy due to electron impact collisions, for instance, recombination of electrons on the dust particle's surface. Further details about the algorithms used to solve the above mentioned equations can be found in [8]. Problems related to the huge difference in the time scale of the dust motion (1–10 s) and the rf period (100 ns) have been solved by time splitting and an iterative procedure. The charge on a dust particle is calculated by using the orbital-motion-limited (OML) probe theory [9]. The charge on the dust particle is assumed to be constant in time during a rf cycle and is obtained from the balance of the local (OML) time-averaged electron and ion currents collected by the particle. Recombination of ions and electrons on the dust particle surface is also taken into account. Ion-neutral collisions have been included to simulate a possible gas heating mechanism. For this we have used a simple approximation by assuming that the energy taken up from the electric field by the ions is dissipated locally in collisions with the gas [10]. We have extended this gas heating mechanism by taking the heating of the dust particle surface into account. The dust particle (surface) temperature can affect the gas temperature, which in turn could affect the other elementary processes in the discharge relevant for the formation of vortices. The thermal balance of the particles can be written as an equality between the thermal influx Q_{in} and the outflux Q_{out}. For a stationary situation the thermal influx is given by $Q_{in} = J_{rec}$, where J_{rec} is the energy flux of the recombining ion and electron flux arriving at the dust particle surface. For a Maxwellian electron energy distribution function, J_{rec} is given by

$$J_{rec} = n_d n_e \sqrt{\frac{k_B T_e}{2\pi m_e}} \exp\left(\frac{eV_{fl}}{k_B T_e}\right)(E_i + eV_{fl}), \tag{8}$$

where T_e is the electron temperature, m_e the electron mass, V_{fl} the floating potential, and E_i the ionization energy, which is 15.7 eV for argon. The outflux is given by $Q_{out} = J_{th} + J_{rad}$. For the pressure range in the PKE experiments, the thermal conduction of the gas J_{th} is governed by the Knudsen theory [11]. J_{rad} is the radiative cooling. J_{th} is given by

$$J_{th} = \frac{\gamma + 1}{16(\gamma - 1)} \frac{p}{\sqrt{T_g}} \sqrt{\frac{8k_B}{\pi m_g}} \alpha (T_p - T_g), \tag{9}$$

where $\gamma = c_p / c_v$ is the heat capacity ratio, m_g the gas molecule mass, p the gas pressure, T_p the dust particle surface temperature, T_g the gas temperature, and α the accommodation coefficient.

The radiative cooling term J_{rad} follows directly from the Stefan-Boltzmann law:

$$J_{rad} = \epsilon \sigma (T_p^4 - T_w^4), \tag{10}$$

where ϵ is the emissivity, σ the Stefan-Boltzmann constant, and T_w the reactor wall temperature. For an argon discharge $\gamma = 5/3$ and $\alpha = 0.86$ have been suggested in the literature [12]. The emissivity of the melamine-formaldehyde particles that are used in the PKE experiments is supposed to be 0.9 [13]. Equation (9) and Eq. (10) are coupled to the temperature balance for the gas and solved with an iterative method.

DUST PARTICLE TRAJECTORIES

In the fluid model [5], the transport of the dust fluid is solved by assuming that the forces acting on the dust particles are in balance with the neutral drag force. In that case the inertia of the dust particles is neglected and a so-called drift-diffusion expression is obtained for the flux of dust particles. This makes the fluid model useful only to study the steady state behavior of dust clouds. To study the vortices that have been seen in the PKE experiments, the inertia and the interaction between the dust particles should be taken into account. The fluid model provides the force field and the linearized Debye length present in a dusty discharge. These are used by the dust particle trajectory model to solve the equation of motion of the dust particles. Neglecting the screened Coulomb interaction with the background dust crystal, the equation of motion is given by

$$m_d \frac{d\vec{v}_d}{dt} = \vec{F}_E + \vec{F}_I + \vec{F}_T + \vec{F}_N + \vec{F}_{SC}, \tag{11}$$

where m_d is the mass of the dust particle, $\vec{v}_d$ its velocity, $\vec{F}_E$ the electric force $\vec{F}_I$ the ion drag force, $\vec{F}_T$ the thermophoretic force, $\vec{F}_N$ the neutral drag force and $\vec{F}_{SC}$ the screened Coulomb force between the dust particles which are tracked in the dust particle trajectory module. For details about the expressions used for the above mentioned forces we refer to previous articles [5,14].

DISCUSSION AND RESULTS

The PKE chamber used by Morfill *et al.* has been modeled. The reactor is cylindrically symmetric. The simulation starts with a zero dust density profile. During the simulation dust is injected from both electrodes by adding source terms in the dust particle balances for the first grid points below and above the electrodes; the injection rate is about 250 000 particles per second. Eventually, a total amount of 0.7 million dust particles is reached; after that the sources are switched off. The electrodes are both driven by a radio frequency power source at a frequency of 13.56 MHz. The peak-to-peak voltage is 70 V. This results in a power dissipation of about 0.04 W. The pressure is 40 Pa. The dust particles have a diameter of 15 μm. The equation of motion for the dust fluid [5] is solved for the time-averaged electric field, plasma densities, and fluxes.

Figure 3 shows the steady state dust density profile. In the center of the discharge a dust-free region, the so-called void, appears, surrounded by a crystalline region of dust with an average density of 1.5×10^{10} m^{-3}.

Figures 4 and 5 show the time-averaged potential distribution $V(r,z)$ in the dust-free and the dusty argon discharges. In both cases the potential has its maximum at the center of the plasma between the electrodes. Comparing the potential distributions, a significant difference in the plasma potential can be observed. The plasma potential decreases in the center of the discharge in the case of a dusty plasma. This shows the importance of taking into account both the contribution of the charge on the dust in the Poisson equation and

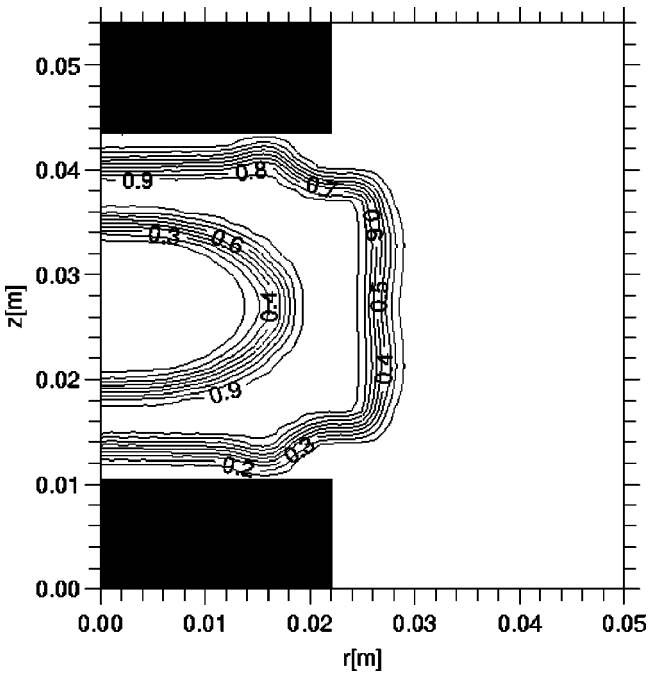

FIG. 3. Simulated dust density profile in an argon discharge, normalized by a factor 1.5×10^{10} m^{-3}.

the recombination on the dust particle surface, which leads to a lower electron density and a higher electron temperature.

Figure 6 shows the gas temperature in a dusty discharge. The gas temperature profile has two maxima of 274.1 K in the sheaths, which is about 1 K higher than the reactor wall temperature, which is kept at 273 K. In the regions where the dust vortices have been observed in the PKE experiments (Fig. 2) the thermal gradient is about 0.1 K/cm. This shows

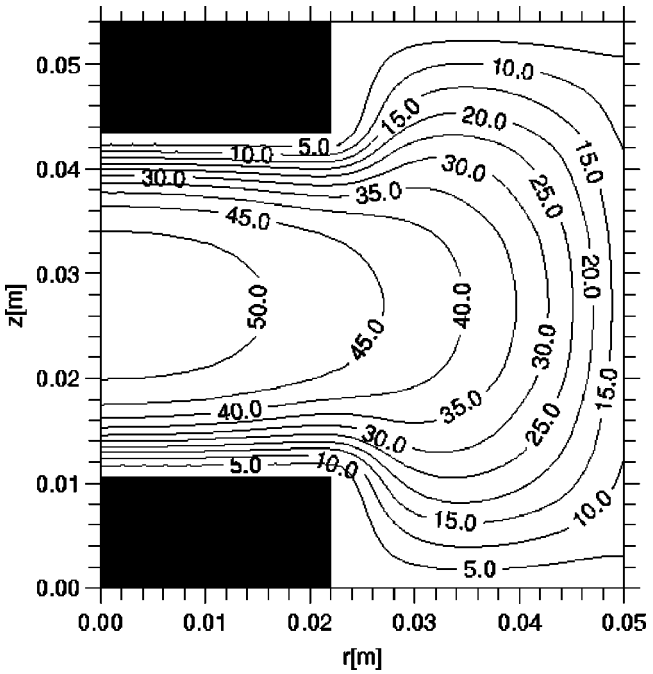

FIG. 4. Time-averaged potential $V(r,z)$ in the dust-free argon discharge.

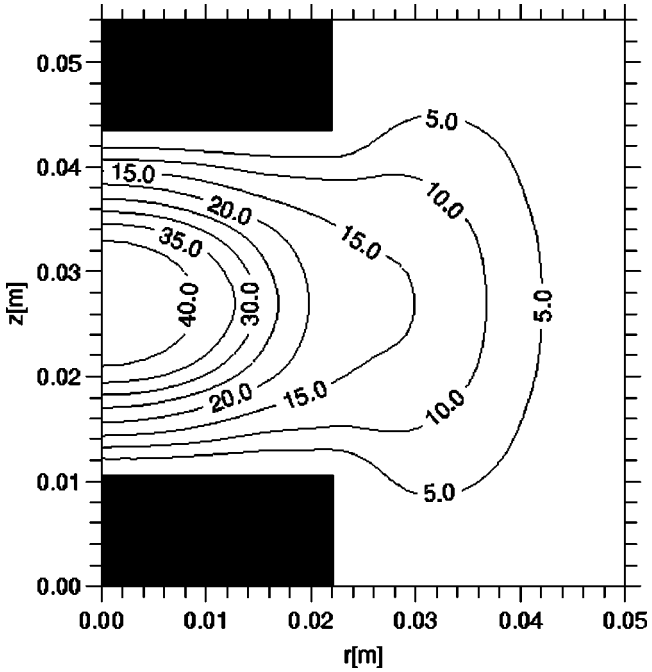

FIG. 5. Time-averaged potential $V(r,z)$ in the dusty argon discharge.

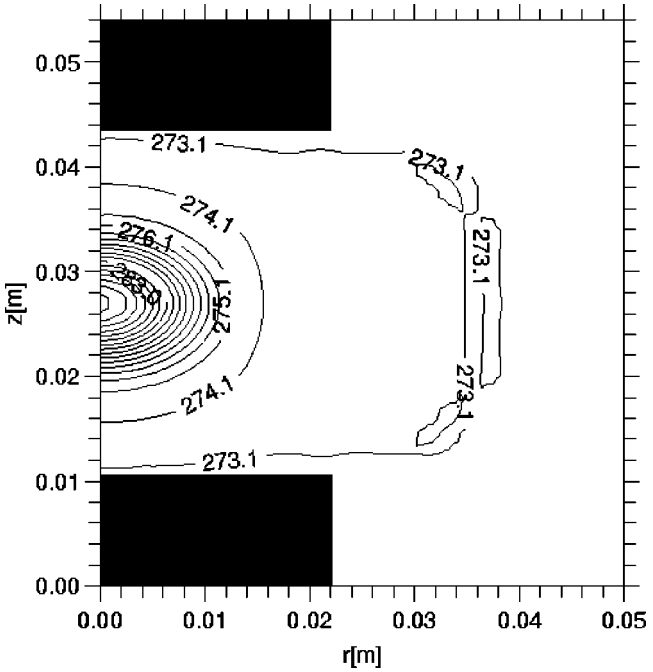

FIG. 7. Dust particle surface temperature in the dusty argon discharge.

that the contribution of the thermophoretic force to the total force on the dust particles is negligible, typically 30 times smaller than the other forces. In Fig. 7 the dust particle (surface) temperature has been plotted. It can be observed that a dust particle would get a maximum temperature in the center of the plasma if it settled there. This is due to the maximum in the ion and electron density in the middle of the discharge, giving a maximum recombination energy flux toward the dust particle surface. Note that the difference between the gas and dust particle temperatures is about 9 K at the center of the discharge.

Figure 8 shows the dust particle trajectories of 12 particles which have been injected from the lower electrode in a dusty argon discharge. Apart from the negligible thermophoretic force (typical value 2×10^{-13} N), the forces acting on a particle are (1) the ion drag force (7×10^{-12} N), which tends to push the particles up or down, away from the plane of symmetry ($z=0.027$), and radially outward, and (2) the electric force (7×10^{-12} N), which acts in the opposite direction. The total force is their sum. At a certain radius in the plane of symmetry (where all axial forces are zero), there is a point where the total radial force becomes zero. This is

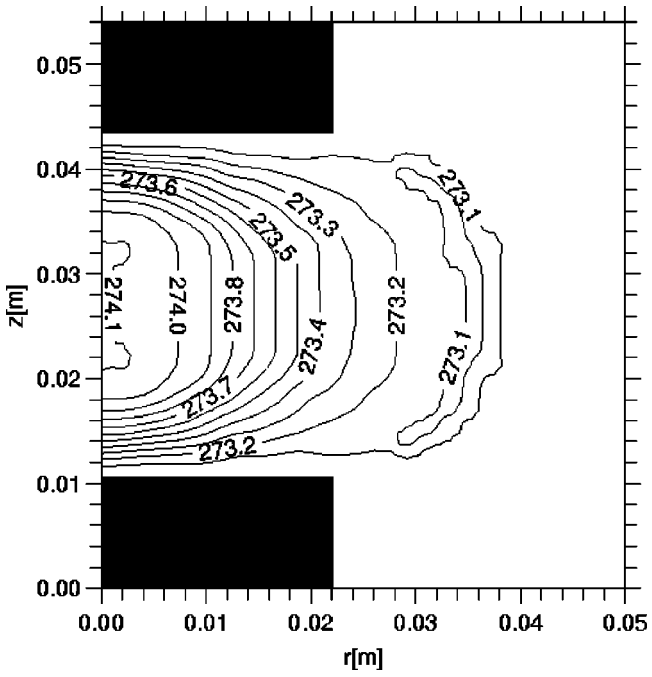

FIG. 6. Gas temperature in the dusty argon discharge.

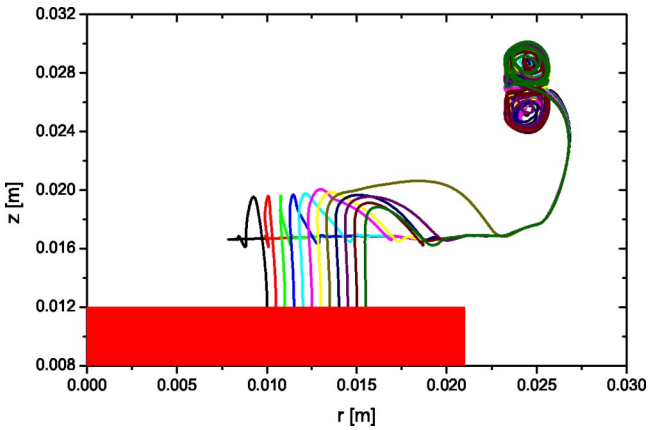

FIG. 8. Trajectories of dust particles injected from the lower electrode in the dusty argon discharge. Two symmetric stable vortices are generated.

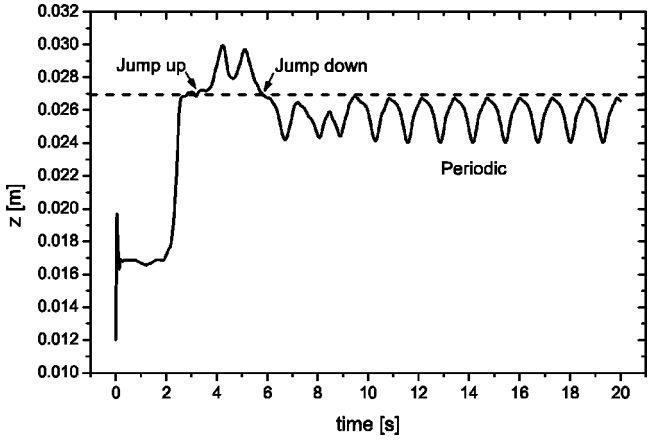

FIG. 9. The axial position of the fourth dust particle injected from the lower electrode at the position $r=0.012$ m as function of time, in the dusty argon discharge. The dashed line is the axial axis of symmetry.

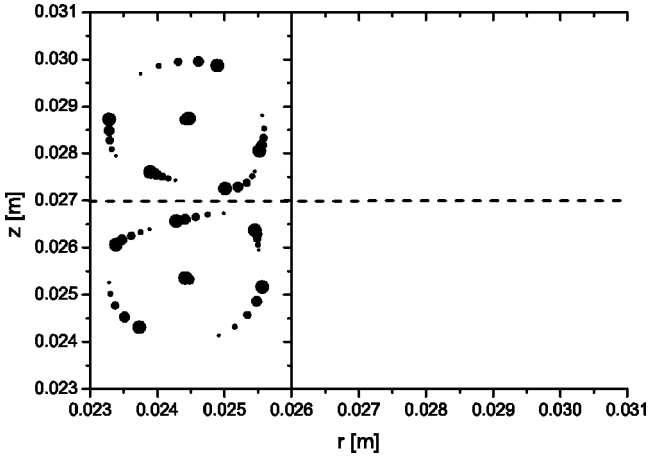

FIG. 10. Positions of dust particles in the dusty argon discharge at different time steps, represented by growing dots. The solid circles show the direction of rotation of the dust cloud. The dashed line is the axial axis of symmetry.

where a single particle will go. The repulsive screened Coulomb force (5×10^{-13} N) prohibits this in the case of more particles. The particles are then forced to stay in the lower or upper half of the reactor and/or inside or outside the radius where the total radial force vanishes. In these regions the total force is not conservative ($\oint \vec{F}_{tot}\cdot\vec{ds}\neq 0$) and the particles start to rotate in the direction dictated by the sign of $\vec{\nabla}\times\vec{F}_{tot}$. The neutral drag force (5×10^{-14} N) causes the particles to move in a closed orbit. These coherent vortices are permanently driven by the forces resulting from the plasma and therefore keep on turning for time scales much longer than the average rotation time. After injection, the system first has an irregular (chaotic) character, where particles can even jump from one cloud to the other (Fig. 9), and then it relaxes toward a self-organized state. Figure 10 shows the dust vortex motion after relaxation in more detail. Each dust cloud consists of six particles, of which five follow the same orbit and one in the middle has a small elliptic orbit. The vortices rotate in opposite directions; this has also been observed in the PKE experiments. The rotation in our case is mainly determined by the combination of ion drag and electric force acting on the dust particles. The ion drag force and the electric force are such that they push the particles axially toward the midplane $z=0.027$ m and radially toward the plane $r=0.0245$ m through the centers of the vortices. The screened Coulomb force, however, keeps the dust particles away from each other. The calculations made by Vaulina *et al.* [3] show that negligible macroparticle charge gradients could cause the dust clouds to rotate. Our calculation shows that no dust charge gradients are needed to get vortices, but that these vortices are driven by the force field dictated by the plasma. The changes in the particle charge in the course of one rotation due to the spatial variation of the plasma parameters are taken into account, but hardly influence its motion. Actually, the gradient in the particle charge is much larger at other positions, outside the vortices. Another difference from the analysis in [3] is the fact that in our case the most dominant forces all depend on the particle charge and gravity is not included.

CONCLUSIONS

The numerical simulation results show that self-consistent modeling of the plasma parameters in a dusty argon discharge is important. Both the contribution of the charge on the dust in the Poisson equation and the recombination on the dust particle surface must be taken into account. The dust-plasma interaction results in a significant difference in the time-averaged potential distributions $V(r,z)$ between a dust-free and a dusty argon discharge. Comparing the gas temperature and dust particle surface temperature in the center of the discharge shows a considerable difference of 9 K, but this does not affect the gas temperature profile. In the region where the dust vortices appear, the thermal gradient of the gas is small; the thermophoretic force is about 30 times smaller than the other forces acting on the dust particles. This fact lets us conclude that the dust vortices are generated by a combination of the ion drag force, electric force, and screened Coulomb force acting on the dust particles and not by the thermophoretic force. Our simulations show good agreement with the PKE experiments done under microgravity.

ACKNOWLEDGMENTS

The authors gratefully acknowledge invaluable discussions with Professor J. Goree (University of Iowa), Professor G. Morfill, Dr. H. Thomas, Dr. A.V. Ivlev (MPI für Extraterrestrische Physik, Garching), and Dr. H. de Blank (FOM-Rijnhuizen). This work was performed under the Euratom-FOM Association Agreement with financial support from the Netherlands Organization for Scientific Research (NWO), the Netherlands Organization for Energy and the Environment (NOVEM), and Euratom.

[1] G. E. Morfill *et al.*, Phys. Rev. Lett. **83**, 1598 (1999).
[2] H. Thomas *et al.*, Phys. Rev. Lett. **73**, 652 (1994).
[3] O. S. Vaulina *et al.*, J. Exp. Theor. Phys. **91**, 1147 (2000).
[4] D. A. Law *et al.*, Phys. Rev. Lett. **80**, 4189 (1998).
[5] M. R. Akdim *et al.*, Phys. Rev. E **65**, 015401(R) (2002).
[6] T. Nitter, Plasma Sources Sci. Technol. **5**, 93 (1996).
[7] P. Belenguer *et al.*, Phys. Rev. A **46**, 7923 (1992).
[8] J. D. P. Passchier *et al.*, J. Appl. Phys. **73**, 1073 (1993).
[9] J. E. Allen *et al.*, J. Plasma Phys. **63**, 299 (2000).
[10] I. Revel *et al.*, J. Appl. Phys. **88**, 2234 (2000).
[11] M. Knudsen, Ann. Phys. (Leipzig) **34**, 539 (1911).
[12] R. Piejak *et al.*, Plasma Sources Sci. Technol. **7**, 590 (1998).
[13] *CRC Handbook of Chemistry and Physics*, 75th ed., edited by David R. Lide (CRC, Boca Raton, FL, 1994).
[14] U. Konopka *et al.*, Phys. Rev. Lett. **84**, 891 (2000).